Materials Research Proceedings 54 (2025) 2047-2057 https://doi.org/10.21741/9781644903599-220

3D printing of soft actuators in nano-filled shape memory thermoplastic polyurethane

Luca Burratti[1,a], Denise Bellisario[2,b*], Fabrizio Quadrini[2,c], Leandro Iorio[1,d] and Loredana Santo[2,e]

[1]Department of Engineering and Science, University "Mercatorum", Rome, Italy

[2]Department of Industrial Engineering, University of Rome "Tor Vergata", Rome, Italy

[a]luca.burratti@uniroma2.it, [b]denise.bellisario@unimercatorum.it, [c]fabrizio.quadrini@uniroma2.it, [d]leandro.iorio@unimercatorum.it, [e]loredana.santo@uniroma2.it

Keywords: Shape Memory Polymers, 3D Printing, Soft Robotics, Smart Materials

Abstract. Today new horizons have opened thanks to the integration of additive manufacturing and shape memory polymers (SMP). Additive manufacturing by fused deposition modelling (FDM) is used to develop new concept soft robotics with SMP. A thermoplastic polyurethane SMP for biomedical uses has been modified by aluminum nanoparticles and multi-walled carbon nanotubes to produce an innovative SMP. The new composite has been extruded to produce the 3D printing wire, which has been used to print a three-dimensional structure. The SM behavior of the composite has been investigated by calorimetry and recovery properties. For comparison the same studies have been carried out to pristine thermoplastic polyurethane. Differential scanning calorimetry, shape fixity and shape recovery ratios, recovery time and recovery force have been investigated for 3D printed structures of pristine and composite samples. The composite demonstrated better results in terms of recovery properties with respect to the pristine material. For this reason, the composite can be a good candidate for soft robotics applications.

Introduction

In recent years, interest and research combining fused deposition modelling with soft robotics have been steadily increasing. This is largely because 3D printing has assisted and enhanced new designs and design logic by incorporating soft materials, thus expanding possibilities and application fields. The ability to produce and utilize soft materials more easily through FDM is accelerating the integration of these additive manufacturing (AM) techniques with the growing interest in soft robots. In fact, soft robots, inspired by nature, mimic living organisms [1]. This type of robot was designed to replace the so-called rigid robots in certain applications, particularly where human interaction is necessary. Soft robots are more compatible for human interactions due to their soft and easily deformable bodies, which minimize damage and impact on both people and the environment [2]. Furthermore, soft robots can adapt to curved and irregular surfaces, a capability that conventional robots lack. These innovative devices can be activated through various mechanisms, such as pneumatic, heat, light, or magnetic activation, further broadening their use across different fields [3–6].

Soft robots have a wide range of applications, spanning from industrial to medical uses. These include human-machine interfaces, locomotion and exploration, manipulation, medical and surgical applications, rehabilitation, and wearable robots. Additionally, space applications are significant; soft robots can perform locomotion in ways that rigid robots cannot, enabling them to navigate and explore unknown terrains. They can move more efficiently and robustly in challenging environments, such as underwater or in space [7], where hard robots struggle. Another innovative application is smart origami structures, which can fold and unfold in response to specific external stimuli, allowing them to reduce in size for transportation or storage [8,9].

Currently, the production of soft robots primarily relies on thermosetting elastomers, such as silicones, which are printed or laminated into 3D structures. AM is often used to create complex hard molds in which the elastomer is transferred and cured. Recently, the use of FDM in soft robotics has expanded with the availability of various flexible materials, including thermoplastics like polylactic acid (PLA) and thermoplastic polyurethanes (TPUs), which are commonly utilized for this purpose [10–13]. These materials are part of the shape memory polymers (SMP) category, capable of returning to their original shape when subjected to thermal stimuli. Their thermoplastic nature also aligns well with fused deposition modeling techniques for producing three-dimensional structures [14]. The combination of smart materials (such as SMPs) and 3D printing leads to what is known as 4D printing (with time as the fourth dimension), where the material changes shape in response to external stimuli, enhancing its functionality for specific applications. 4D printing (4DP) distinguishes itself as a cutting-edge technology in contrast to conventional 3D-printed components, which are renowned for their rigidity and static nature [15,16]. The possibility of dynamic shape-shifting in AM techniques has emerged as a key area of investigation [17]. Recently, TPU has been modified by adding nanomaterials to improve its shape memory performance. The materials used for this purpose include metallic nanoparticles, metal oxide nanoparticles, and carbon-based nanomaterials, such as graphene oxide and carbon nanotubes [18–22]. Indeed, the presence of these nanomaterials can change the mechanical, thermal and recovery properties.

In this work, a new TPU composite was synthetized and used to produce 3D printed structures with SM properties. Commercial TPU pellets are used in combination with aluminum nanoparticles (AlNPs) and multi-walled carbon nanotubes (CNTs) to produce a composite with a total percentage of fillers equal to 3% in weight. Subsequently, a filament for the FDM is produced and used to print a 3D structure with shape memory properties, to achieve a 4DP process. This composite was compared with the pristine TPU to validate the possibility of fabricating soft robots' parts. In this regard, specific structures with the possibility of embedding a microheater were designed and printed. Thermal properties, shape recovery properties, temperatures and times of these 4DP structures were investigated.

Materials and methods

Materials. Commercial thermoplastic polyurethane (TPU) pellets (DiAPLEX MM3510) were acquired from SMP Technologies Inc (Japan), multi-walled carbon nanotubes (CNTs, outer diameter < 8 μm, length 10-30 μm, purity > 95 wt% and ash < 1.5 wt%) were purchased from CHEAPTUBES.COM and aluminum nanoparticles (AlNPs, diameter 40-60 nm) were obtained from US Research Nanomaterials. The products were used as received, without any purification process. Microheaters (model KHLVA – 0502/10, 10 W/in2 maximum 28 V) were acquired from Omega Engineering.

Manufacturing of TPU composite. Brabender (Plastograph) was used as a laboratory mixer to synthesise the TPU composite. In a typical synthesis, 20 g of TPU pellets are introduced into the machine at the temperature of 150 °C and mixed for 3 minutes at the rotation speed of 50 rpm. After that, 0.5 g of CNTs and 0.1 g of AlNPs (with a 5:1 ratio) were added to the TPU and mixed for another 7 minutes. The final mass percentage of the nanomaterials was 3% with the ratio CTNs/AlNPs equal to 5/1. For comparison, the pure TPU pellets were mixed with the following parameters: 150 °C, 5 minutes, and 50 rpm. At the end of the mixing process, the samples were manually cut into small parts of a few mm3 (pellets).

3D printing filament production. The filament was produced by a filament maker (3DEVO Composer 450). The machine has a hopper (volume 2l) for pellets introduction, four heating zones (with a maximum temperature of 450°C) and a single screw extruder (with a rpm range from 2 to 15). A spooling system that adjusts the speed according to the measured diameter is also present and two fans for cooling at the outlet of the nozzle. Several tests were performed in order to

optimize the processing parameters, and the optimized ones are reported in Table 1. The filament diameter was 1.75 ± 0.1 mm. The extruded polymer is collected and automatically wrapped around a coil.

Table 1 – Optimized parameters for filament production.

		
Heating zone temperature	1	170 °C
	2	190 °C
	3	195 °C
	4	193 °C
Extruder speed	3.7 rpm	
Fan speed	80%	

Sample fabrication. The process of fabricating samples began with designing a structure that would be useful for testing. The printed samples were designed to have dimensions of 16x50x2.6 mm^3 and a unique slot of 14x50x0.4 mm^3. The slot is designed to fit within the limitations of a 3D printer and to have a useful size for inserting the microheater. Moreover, the geometry was designed to have homogeneous and effective heating of the sample. The design of the final structure is reported in Figure 1a and 1b with the dimensions. The Figure 1c and 1d represent the final 3D structures without and with microheater, respectively.

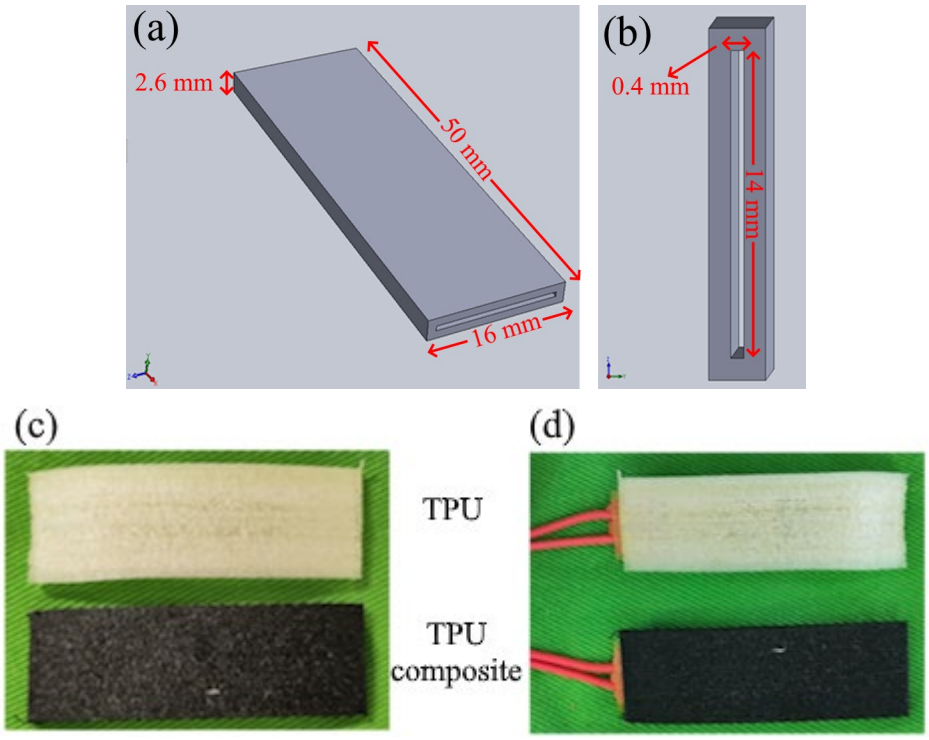

Figure 1 – Images of the designed structures, front angular view (a) and cross section view (b); pictures of the printed samples without (b) and with (c) microheater.

Materials Research Proceedings 54 (2025) 2047-2057 https://doi.org/10.21741/9781644903599-220

The samples were printed using a commercial Fused Deposition Modelling (FDM) printer (Prusa i3 MK3S+, Prusa Research, Czech Republic). Fig. 2 illustrates how the samples have been oriented on the printing bed to optimize the 3D printing phase. The used printing parameters are reported in Table 2. Some parameters are optimized such as nuzzle temperature (210 – 240 °C), nuzzle diameter (0.2 - 0.4 - 0.8 mm) and printing speed (20 – 40 mm/s).

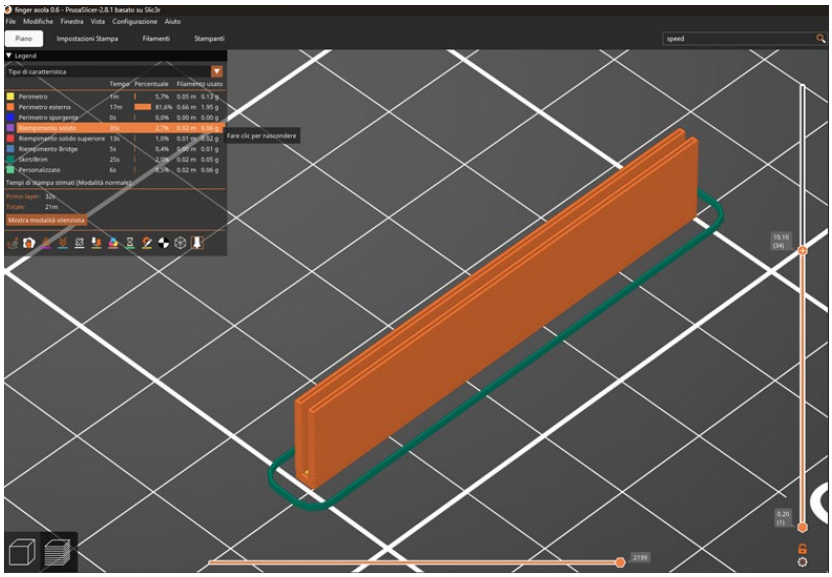

Figure 2 – Screenshot of the Prusa slicer software with the specific orientation of the sample for the printing phase.

Table 2 – FDM printing parameters.

Nozzle temperature	220 °C (240°C)*
Nozzle diameter	0.4 mm
Printer bed temperature	50°C
Printing speed	40 mm/s
Infill	100%
Pattern	linear
Raster angle	45°
Layer thickness	0.3 mm
Retraction length	0.8 mm

* for pristine TPU

Differential scanning calorimetry. Small samples of specimens were also used for differential scanning calorimetry (DSC6, Perkin Elmer) which is a useful technique to investigate thermal behavior of TPU composites. Double scans were carried out from -5 to 200°C at 10 °C/min. The measurements were carried out in a nitrogen atmosphere. T_g was calculated for all samples.

Shape fixity ratio, shape recovery ratio and recovery time. Once placed the microheater inside the samples (pristine TPU and TPU composite), they were heated above the T_g for 5 minutes and fixed around a cylinder by using adhesive tape (step 1). Subsequently, the samples were cooled below the T_g in a fridge (-22 °C, step 2) and then the samples were heated again (step 3). During the heating (step 3) the samples were fixed with a clamp, and a video was recorded for extrapolating the information about the angles to calculate the shape fixity ratio (R_f) and shape recovery ratio (R_r). The camera was fixed perpendicularly to the samples in order to record in the same position all the samples, avoiding angle aberration. The R_f and R_f were measured according to the Eqs. 1 and 2 [23]:

$$R_f = (180° - \theta_1)/(180° - \theta_0)*100 \quad (1)$$

$$R_r = (\theta_2 - \theta_1)/(180°- - \theta_1)*100 \quad (2)$$

where, $\theta_0 = 0$, θ_1 and θ_2 represent the angles that the samples have at the beginning and at the end of the recovery test, respectively. A schematic representation is shown in Fig. 3.

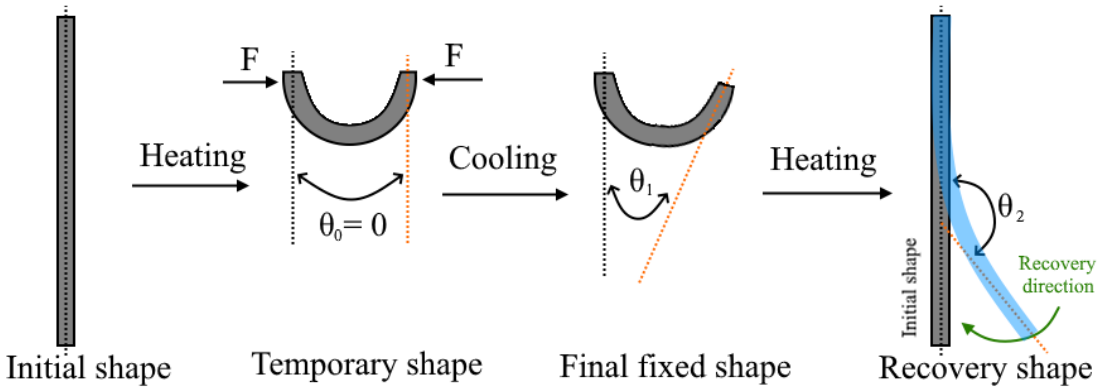

Figure 3 – Schematic representation of fixity and recovery measurements.

The experiment was carried out by using three different voltages applied to the microheater, 6 V, 9 V and 12 V, for each voltage the R_f and R_r values were calculated.

The recovery time for each sample was extrapolated from the videos of Rf and Rr tests.

Recovery force measurements. The recovery force tests were accomplished by universal testing machine (Insight 5, MTS System Corp.), the samples were memorized in the shape as in the case of the determination of R_f and R_r ratios. The sample was placed between two compression plates (Fig. 4), the microheater was connected to the power supply and the force exerted by the sample on the load cell (nominal maximum load 100 N, MTS System Corp.) was recorded. For each voltage, the experiment was repeated three times. From the spectra recorded, the plateau values of the three replicas were averaged and normalized by the mass of the sample.

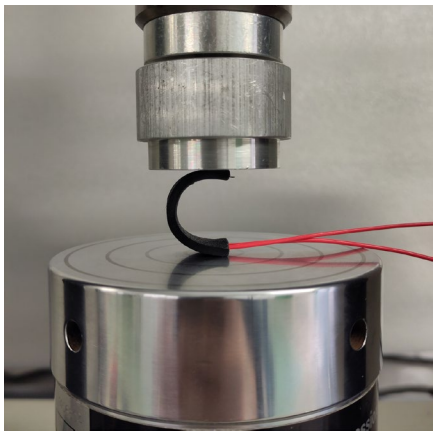

Figure 4 – Picture of the recovery force test experimental set-up.

Results and discussion

Thermal analysis. Fig. 5 shows the DSC thermograms of the unfilled TPU and TPU composite samples from Brabender mixer, respectively. Both samples with and without nanofillers were scanned two times and the second scans are reported. All DSC curves have been normalized. Table 3 reports the glass transition temperature T_g and the melting peak T_m extracted from all the DSC curves. The Figure 5 shows the normalized heat flow as a function of temperature for the pristine

TPU (black line) and composite (red curve), the inset represents a portion of the DSC spectrum in correspondence of the melting temperature (T_m). Main transitions in the DSC scans refer to the glass transition of the soft segments, tailored about 35°C, and the melting point of the hard segments (over 150°C). Small curves anomalies between these 2 points (about 100°C) may refer to the glass transition of the hard segments but are not very clear. There is a slight decrease in T_g in the TPU composite. The main reason for this phenomenon is that the entanglement degree of the soft segment molecules of TPU may be reduced in the presence of filler, causing the higher mobility of soft segments. As expected, because of the interaction of the nanofillers with the polymer matrix, molecular mobility in the melt is reduced with the effect of a decrease of the glass transition and a reduction of the crystallization extent. Moreover, destroying the crystalline structure of hard segments, which act as physical crosslinking points for TPU molecules, will release the constrained soft segments and increase their mobility, which will lead to a decrease in T_g. In fact, nanofillers can show an increased tendency towards agglomeration and this agglomeration can also introduce a lubrication action on molecular mobility. Therefore, the agglomeration of nanofiller caused T_g of TPU composite to be lower than that of the neat matrix material [24].

The T_m value for the TPU composite was around 179°C, as shown in the Table 3. However, the melting peak of the pristine TPU is shifted with the presence of the nanofillers. Therefore, the result of fillers into the matrix is a slight increase of the melting temperature of TPU.

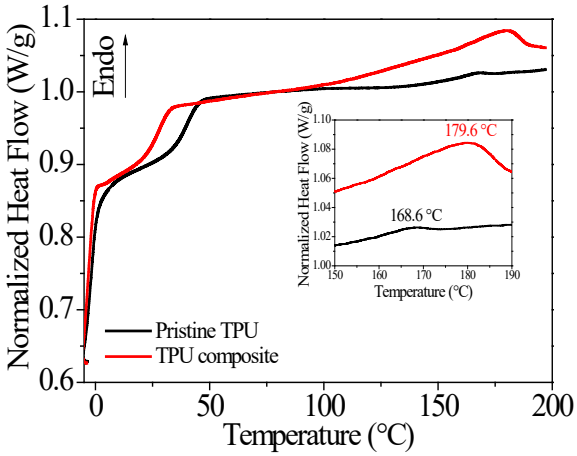

Figure 5 – DSC spectra (second scan) of synthesized samples; insets represent the melting peaks of the samples.

Table 3 – Glass transition temperature (T_g) and melting temperature (T_m) of the samples.

Sample	T_g (°C)	T_m (°C)
Pristine TPU	34.9	168.6
TPU Composite	27.8	179.6

Recovery performances. A polymer's shape memory behavior depends on the presence of two phases: a crystalline phase (physical net points, also known as hard segments) that plays a fixed role in TPU, and a changeable phase connected to the transition temperatures (soft segments). The polymer is programmed in a shape below the glass transition temperature, and the soft segments are frozen. The specimen releases stress, and the soft chains revert to their initial shape when the sample is heated over the Tg. Conversely, the dynamics, free volume, physical and chemical

interactions, and crystallinity of soft segments in TPU are responsible for the shape recovery and fixity characteristics. This means that the hard and soft segments of the TPU system are related to the change from the fixed phase to the reversible phase.

To establish more precisely the temperatures reached by the TPU samples as a function of the heating conditions by means of a microheater, preliminary tests have been carried out. So, the temperature of the samples as a function of applied voltage and heating time was studied. A thermocouple was fixed on the surface of the samples (pristine TPU or TPU composite), the voltage was applied to the microheater and the temperature of the thermocouple was recorded in the range time from 0 to 5 minutes with a data acquisition module (Omega Engineering, TC-08). The temperature of the sample surface is displayed in Fig. 6 as a result of time at different applied voltages. After 5 minutes, the temperature reached by the samples is different and depends on the applied voltage. Increased voltage increases the final temperature of the sample.

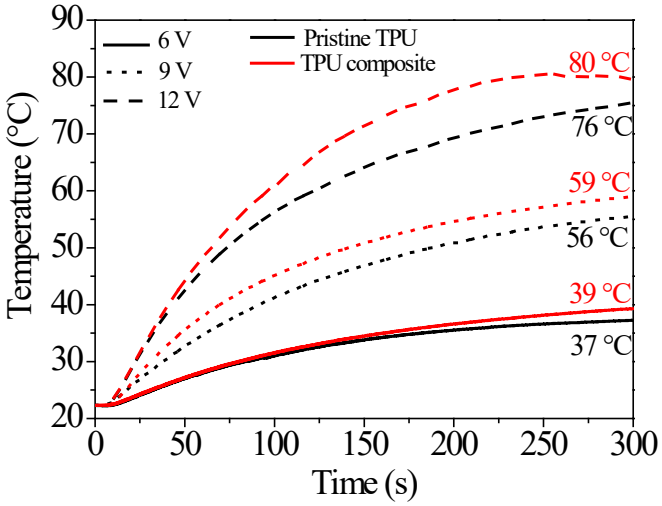

Figure 6 – Temperature on the samples surface as a function of time: black lines represent the pristine TPU, while red lines refer to the TPU composite. Solid curves are the measurements at 6 V, dotted lines at 9 V and dashed lines at 12 V.

The same voltages were used for the shape memory evaluation phases of the pristine and composite TPU samples. Table 4 lists the initial (θ_1) and final (θ_2) angles with the R_f and R_r ratios for each sample at different applied voltage. By increasing the applied voltage, the θ_1 of pristine TPU decreases from 35.4° (6 V) to 8.8° (12 V). Consequently, the heat provided by the microheater at 6 V and 9V is not sufficient to adequately fix the shape of the sample. On the contrary, 12 V ensures sufficient heat to minimize the angle θ_1. The same trend is found for the TPU composite, where θ_1 passed from 16.60° (6 V) to 5.30° (12 V). In general, the θ_1 values are lowest for TPU composite. The presence of the AlNPs and CNTs improved the heat transmission and ensured a better fixity ratio even at low voltages and thus a better shape memory programming. The recovery properties are related to the θ_2 values, the greater the angle the greater the sample recovery. For the pristine TPU, an increase of the R_r value is recorded (from 53% to 69%), by changing from 6 V to 12 V. Also in this case, the higher voltage applied to the microheater produces sufficient heat to achieve the maximum shape recovery. Considering the TPU composite, the R_r value is high already at 6 V (93%), but the sample suffers from cycling and consequently the R_r value at 12 V is slightly lower (88%). Finally, the TPU composite displayed a remarkable increase of the shape memory properties. As an example, in Figure 7 are shown the final fixed shape (a) and recovery shape (b) phases of the TPU composite sample at an applied voltage of 6 V.

Table 4 – Initial and final angles for the recovery tests, the R_f and R_r values and recovery time for each investigated sample.

Sample	θ_1 (°)	θ_2 (°)	R_f (%)	R_r (%)	Recovery time (s)
TPU 6 V	35.4	112.4	80	53	271
TPU composite 6 V	16.6	168.6	91	93	251
TPU 9 V	19.1	123.6	89	65	241
TPU composite 9 V	16.4	167.8	91	93	238
TPU 12 V	8.8	127.3	95	69	240
TPU composite 12 V	5.3	158.9	97	88	210

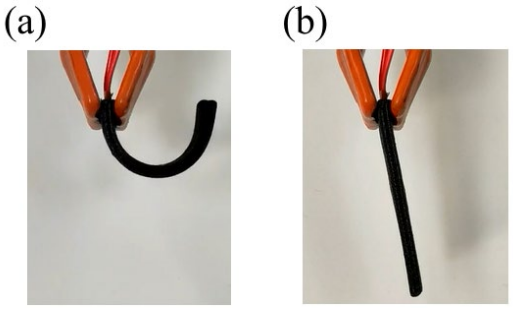

Figure 7. – Final fixed shape (a) and recovery shape (b) phases for the TPU composite sample with a voltage applied of 6 V.

Last column of the Table 4 shows the recovery time of the samples, the presence of the fillers boosts the recovery speed, from 240 seconds in the pristine TPU to 210 seconds for the composite (12 V applied).

The recovery force tests are depicted in the

Figure 8. Regardless of the applied voltage, all the composite samples exhibit a recovery force per unit mass of about 4 times greater than the samples without fillers.

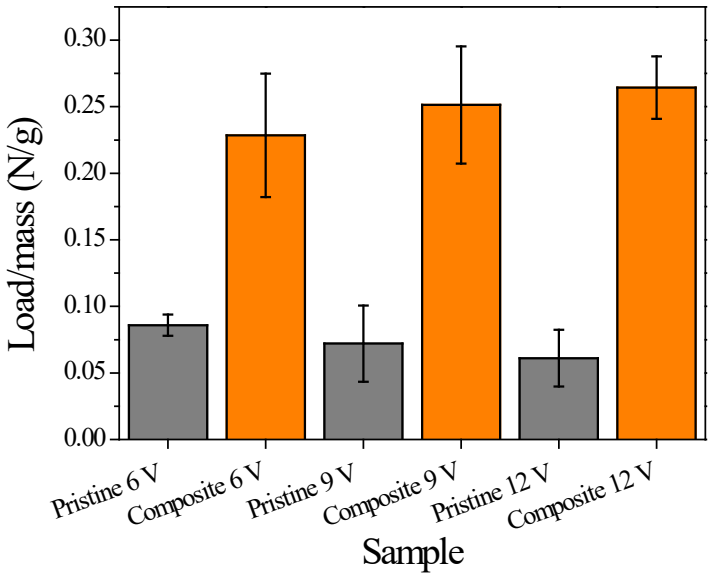

Figure 8 – Force per unit mass as a function of voltage applied; grey bar refers to pristine TPU samples, while orange bars represent composite samples.

Conclusions

Herein, this study presented the fabrication and the heat-actuated shape memory properties of a TPU composite that was produced by incorporating 3% wt. of aluminum nanoparticles (AlNPs) and multi-walled carbon nanotubes (CNTs) with a ratio CNTs:AlNPs equal to 5:1. The composite was used to produce a filament for FDM and subsequently a 3D structure with SMP was printed. The 3D sample had a rectangular slot for inserting a microheater. For comparison the same 3D structure was printed also using pristine TPU. We found that the fillers extended shape memory properties of pristine TPU. The best heat-actuated shape recovery (88%) and fixity (97%) performance were achieved by using an applied voltage of 12 V to the microheater. In addition, the recovery time decreased from 240 to 210 seconds using the TPU composite. These results highlight that the TPU composite can be a good candidate for use within soft robotics, as it maintains the soft characteristics of TPU but enhances the shape memory properties. Further investigations must be made into the multi-cycling SM behavior of the TPU composite structure.

Acknowledgments

This paper and the research behind it would not have been possible without the exceptional support of our laboratory technician, Fabrizio Betti. This study was carried out within the “4D Printing of smart soft robotics (4D P.Ro.)” and received funding from the Research Projects of Significant National Interest (PRIN) 2022 PNRR, project n. 2022SFF349, with CUP Master D53D23004020008.

References

[1] Q. Zhao, Sensing Materials: Bio-inspired materials. in: R. Narayan, (Ed), Encyclopedia of sensors and biosensors; Elsevier, 2023 435–444.

[2] C. Majidi, Soft Robotics: A perspective - current trends and prospects for the future. Soft Robot. 1 (2014) 5–11. https://doi.org/10.1089/soro.2013.0001

[3] D. Gonzalez, J. Garcia, R. M. Voyles, R.A. Nawrocki, B. Newell, Characterization of 3D printed pneumatic soft actuator. Sens. Actuators A: Phys., 334 (2022) 113337. https://doi.org/10.1016/j.sna.2021.113337

[4] Z. Ji, P. Jiang, R. Guo, K. R. Hossain, X. Wang, 4D-printed light-responsive structures. in: M. Bodaghi, A. Zolfagharian, (Eds), Smart materials in additive manufacturing, Volume 1 : 4D printing principles and fabrication; Elsevier, 2022. 55–105.

[5] Y. Kim, X. Zhao, Magnetic soft materials and robots. Chem. Rev. 122 (2022) 5317–5364. https://doi.org/10.1021/acs.chemrev.1c00481

[6] M. Y. Khalid, Z.U. Arif, A. Tariq, M. Hossain, K. Ahmed Khan, R. Umer, 3D printing of magneto-active smart materials for advanced actuators and soft robotics applications. Eur. Polym. J. 205 (2024) 112718. https://doi.org/10.1016/j.eurpolymj.2023.112718

[7] C. Lee, M. Kim, Y.J. Kim, N. Hong, S. Ryu, H.J. Kim, S. Kim, Soft robot review. Int. J. Control. Autom. Syst 15 (2017) 3–15. https://doi.org/10.1007/s12555-016-0462-3

[8] Z. Chen, Y. Li, Q. M. Li, Hydrogel-driven origami metamaterials for tunable swelling behavior. Mater. Des. 207 (2021) 109819. https://doi.org/10.1016/j.matdes.2021.109819

[9] S. Chen, J. Chen, X. Zhang, Z.-Y. Li, J. Li, Kirigami/origami: unfolding the new regime of advanced 3D microfabrication/nanofabrication with “folding.” Light Sci. Appl. 9 (2020) 75. https://doi.org/10.1038/s41377-020-0309-9

[10] Y. Yang, Y. Chen, Y. Wei, Y Li, 3D printing of shape memory polymer for functional part fabrication. Int. J. Adv. Manuf. Technol. 84 (2016) 2079–2095.

https://doi.org/10.1007/s00170-015-7843-2

[11] J. Wang, Z. Wang, Z. Song, L. Ren, Q. Liu, L. Ren, Biomimetic shape–color double-responsive 4D printing. Adv. Mater. Technol. 4 (2019). https://doi.org/10.1002/admt.201900293

[12] M. Ramezani, M. B. B. Monroe, Biostable segmented thermoplastic polyurethane shape memory polymers for smart biomedical applications. ACS Appl. Polym. Mater. 4 (2022) 1956–1965. https://doi.org/10.1021/acsapm.1c01808

[13] N. Sabahi, I. Roohani, C. H. Wang, E. Farajzadeh, X. Li, Thermoplastic polyurethane-based shape memory polymers with potential biomedical application: The effect of TPU soft-segment on shape memory effect and cytocompatibility. Polymer 283 (2023) 126189. https://doi.org/10.1016/j.polymer.2023.126189

[14] S. Walker, O. D. Yirmibeşoğlu, U. Daalkhaijav, Y. Mengüç, Additive manufacturing of soft robots in: S.M. Walsh, M.S. Strano, (Eds.), Robotic systems and autonomous platforms; Elsevier, 2019 335–359.

[15] M. H. Yousuf, W. Abuzaid, M. Alkhader, 4D printed auxetic structures with tunable mechanical properties. Addit. Manuf. 35 (2020) 101364. https://doi.org/10.1016/j.addma.2020.101364

[16] K. McLellan, Y.-C. Sun, H. E. Naguib, A review of 4D printing: materials, structures, and designs towards the printing of biomedical wearable devices. Bioprinting 27 (2022) e00217. https://doi.org/10.1016/j.bprint.2022.e00217

[17] S. B. Kumar, J. Jeevamalar, P. Ramu, G. Suresh, K. Senthilnathan, Evaluation in 4D printing – A review. Mater. Today Proc. 45 (2021) 1433–1437. https://doi.org/10.1016/j.matpr.2020.07.335

[18] X. Xu, P. Fan, J. Ren, Y. Cheng, J. Ren, J. Zhao, R. Song, Self-healing thermoplastic polyurethane (TPU)/polycaprolactone (PCL) /multi-wall carbon nanotubes (MWCNTs) blend as shape-memory composites. Compos. Sci. Technol. 168 (2018) 255–262. https://doi.org/10.1016/j.compscitech.2018.10.003

[19] D. Xiang, X. Zhang, E. Harkin-Jones, W. Zhu, Z. Zhou, Y. Shen, Y. Li, C. Zhao, P. Wang, Synergistic effects of hybrid conductive nanofillers on the performance of 3D printed highly elastic strain sensors. Compos. Part A Appl. Sci. Manuf. 129 (2020) 105730. https://doi.org/10.1016/j.compositesa.2019.105730

[20] M. Abrisham, M. Panahi-Sarmad, G. Mir Mohamad Sadeghi, M. Arjmand, P. Dehghan, A. Amirkiai, Microstructural design for enhanced mechanical property and shape memory behavior of polyurethane nanocomposites: Role of carbon nanotube, montmorillonite, and their hybrid fillers. Polym. Test. 89 (2020) 106642. https://doi.org/10.1016/j.polymertesting.2020.106642

[21] Y. Guo, L. Yan, Z. Zeng, L. Chen, M. Ma, R. Luo, J. Bian, H. Lin, D. Chen, TPU/PLA nanocomposites with improved mechanical and shape memory properties fabricated via phase morphology control and incorporation of multi-walled carbon nanotubes nanofillers. Polym. Eng. Sci. 60 (2020) 1118–1128. https://doi.org/10.1002/pen.25365

[22] M. Panahi-Sarmad, V. Goodarzi, A. Amirkiai, M. Noroozi, M. Abrisham, P. Dehghan, Y. Shakeri, N. Karimpour-Motlagh, F. Poudineh Hajipoor, H. Ali Khonakdar, A. Asefnejad, Programing polyurethane with systematic presence of graphene-oxide (GO) and reduced graphene-oxide (rGO) platelets for adjusting of heat-actuated shape memory properties. Eur. Polym. J. 118 (2019) 619–632. https://doi.org/10.1016/j.eurpolymj.2019.06.034

[23] B. Liu, X. Gu, X. Chen, Y. Yang, J. Zou, H. Yin, Y. Cai, Preparation, shape memory properties and application research of PLA/PCL-based shape memory polymers doped with Al2O3 and lignin. J. Appl. Polym. Sci. 141 (2024) doi:10.1002/app.55252

[24] J. Zhu, C. Abeykoon, N. Karim, Investigation into the effects of fillers in polymer processing. Int. J. Light. Mater. Manuf. 4 (2021) 370–382. https://doi.org/10.1016/j.ijlmm.2021.04.003